

# The Galaxy Population of Low-Redshift Abell Clusters

Wayne A. Barkhouse,<sup>1,4</sup> H.K.C. Yee,<sup>2,4</sup> and Omar López-Cruz<sup>3,4</sup>

## ABSTRACT

We present a study of the luminosity and color properties of galaxies selected from a sample of 57 low-redshift Abell clusters. We utilize the non-parametric dwarf-to-giant ratio (DGR) and the blue galaxy fraction ( $f_b$ ) to investigate the clustercentric radial-dependent changes in the cluster galaxy population. Composite cluster samples are combined by scaling the counting radius by  $r_{200}$  to minimize radius selection bias. The separation of galaxies into a red and blue population was achieved by selecting galaxies relative to the cluster color-magnitude relation. The DGR of the red and blue galaxies is found to be independent of cluster richness ( $B_{gc}$ ), although the DGR is larger for the blue population at all measured radii. A decrease in the DGR for the red and red+blue galaxies is detected in the cluster core region, while the blue galaxy DGR is nearly independent of radius. The  $f_b$  is found not to correlate with  $B_{gc}$ ; however, a steady decline toward the inner-cluster region is observed for the giant galaxies. The dwarf galaxy  $f_b$  is approximately constant with clustercentric radius except for the inner cluster core region where  $f_b$  decreases. The clustercentric radial dependence of the DGR and the galaxy blue fraction, indicates that it is unlikely that a simple scenario based on either pure disruption or pure fading/reddening can describe the evolution of infalling dwarf galaxies; both outcomes are produced by the cluster environment.

*Subject headings:* galaxies: clusters: general — galaxies: luminosities: colors — galaxies: dwarf — galaxies: formation — galaxies: evolution

---

<sup>1</sup>Department of Physics and Astrophysics, University of North Dakota, Grand Forks, ND 58202; email: wayne.barkhouse@und.nodak.edu

<sup>2</sup>Department of Astronomy and Astrophysics, University of Toronto, Toronto, ON, Canada, M5S 3H8; email: hyee@astro.utoronto.ca

<sup>3</sup>Instituto Nacional de Astrofísica, Óptica y Electrónica, Tonantzintla, Pue., México; email: omarlx@inaoep.mx

<sup>4</sup>Visiting Astronomer, Kitt Peak National Observatory. KPNO is operated by AURA, Inc. under contract to the National Science Foundation.

## 1. Introduction

A fundamental goal in the study of galaxy clusters is to understand the role of environment on galaxy formation and evolution. The well-established morphology–density relation (e.g., Dressler 1980; Dressler et al. 1997; Thomas & Katgert 2006) highlights the impact of location on the properties of cluster galaxies: the cores of rich clusters are inundated with early-type galaxies while the outskirts contain a large fraction of late-type systems (for example, see Abraham et al. 1996; Morris et al. 1998; Treu et al. 2003; Smith et al. 2006).

A theoretical understanding of the morphology–density relation has focused on the influence of dynamical factors on the formation of early-type galaxies in high-density regions via the merger of late-type galaxies (e.g., Okamoto & Nagashima 2001). Mergers are expected to occur with greater ease in areas where the galaxy velocity dispersion is low (e.g., Merritt 1984). This is in contrast to the high-velocity dispersion regions found at the center of rich clusters (e.g., Rood et al. 1972; Kent & Gunn 1982; Dubinski 1998). To solve this apparent contradiction with the observed morphology–density relation, it is hypothesized that the transformation of late- into early-type galaxies occurred in group-like environments with a low-velocity dispersion, as clusters assembled from the gravitational infall of matter (e.g., Roos & Norman 1979; McIntosh et al. 2004). Once a cluster has formed, other dynamical processes, such as galaxy harassment and ram pressure stripping, will determine the current morphological makeup of the cluster galaxy population (Moore et al. 1996; Abadi et al. 1999; Quilis et al. 2000; Boselli & Gavazzi 2006).

In general, low-redshift clusters contain two major galaxy populations; a red, evolved, early-type component that dominates the central cluster region, and a blue, late-type population which has undergone relatively recent star formation and is most prominent in the outskirts of clusters (for example, see Abraham et al. 1996; Wake et al. 2005; Wolf et al. 2007). This has led to the hypothesis that clusters are built-up gradually from the infall of field galaxies (e.g., Ellingson et al. 2001; Treu et al. 2003; McIntosh et al. 2004).

Understanding how different sub-populations of galaxies evolve in clusters can be further elucidated by subdividing the cluster galaxy population with respect to luminosity and color. Barkhouse et al. (2007, hereafter B07) demonstrated that, in general, the faint-end slope of the cluster luminosity function (LF) becomes steeper with increasing clustercentric distance. In this paper we examine the radial dependence of galaxy luminosity by measuring the dwarf-to-giant ratio (DGR) as a function of clustercentric radius. Unlike the galaxy LF, the non-parametric DGR provides a robust measure of the relative fraction of faint-to-bright galaxies without assuming a specific functional form for the LF. In López-Cruz et al. (2004) we presented evidence for a blueward shift in the color-magnitude relation (CMR) with increasing clustercentric radius, utilizing the same cluster sample as this paper. To quantify

changes in galaxy color as a function of clustercentric radius, we search for radius-dependent changes in the blue galaxy fraction ( $f_b$ ).

This paper is the third in a series resulting from a large multi-color imaging survey of low-redshift Abell galaxy clusters. This paper is organized as follows. In §2 we briefly summarize the sample selection criteria, observations, and photometric reductions. In §3 we examine the dwarf-to-giant ratio, while the blue galaxy fraction is explored in §4. We compare our findings with published results in §5 and discuss our findings in §6. Finally we summarize our conclusions in §7.

Further details regarding sample selection, observations, image preprocessing, catalogs, and finding charts can be found in López-Cruz (1997), Barkhouse (2003), López-Cruz et al. (2004), and O. López-Cruz et al. (2009, in preparation). The investigation of the color-magnitude relation for this cluster sample is presented in Paper I (López-Cruz et al. 2004), while the galaxy cluster LFs are presented in Paper II (B07).

Due to the low redshift nature of our cluster sample ( $z < 0.2$ ), the effects of curvature and dark energy are negligible. To allow a direct comparison with previous studies, we use  $H_0 = 50 h_{50} \text{ km s}^{-1} \text{ Mpc}^{-1}$  and  $q_0 = 0$ , unless otherwise indicated.

## 2. Observations and Data Reductions

We present in this section a brief summary of the cluster sample selection criteria, observations, data reductions, and photometric measurements. We refer the reader to López-Cruz (1997), Barkhouse (2003), López-Cruz et al. (2004), and B07 for further details.

The Abell clusters in our sample are selected mainly from the catalog of *Einstein*-detected bright X-ray clusters compiled by Jones & Forman (1999). This sample includes 47 clusters observed at KPNO using the 0.9 m telescope plus the T2kA ( $2048 \times 2048$  pixels;  $0.68'' \text{ pixel}^{-1}$ ) CCD detector (the LOCOS sample; López-Cruz 1997; Yee & López-Cruz 1999; López-Cruz 2001, O. López-Cruz et al. 2009, in preparation). These clusters were chosen to be at high galactic latitude ( $|b| \geq 30^\circ$ ) and within the redshift range of  $0.04 \leq z \leq 0.20$ . To probe the low redshift regime ( $0.02 \leq z \leq 0.04$ ), eight clusters imaged using the KPNO 0.9 m + MOSAIC 8K camera ( $8192 \times 8192$  pixels;  $0.423'' \text{ pixel}^{-1}$ ) from Barkhouse (2003) were incorporated in our sample. In addition, two clusters from Brown (1997) using the same instrumental setup as the LOCOS sample and selection criteria as the mosaic data are included.

The integration times for our 57-cluster sample varies from 250 to 9900 s, depending

on the filter ( $B$  or  $R_C$ ) and the redshift of the cluster. For this study we use a total of five control fields, which were chosen at random positions on the sky at least  $5^\circ$  away from the clusters in the sample. These control fields were observed using the MOSAIC camera to a comparable depth and reduced in the same manner as the cluster data.

Preprocessing of the images was done using IRAF and photometric reductions were carried out using the program PPP (Picture Processing Package; Yee 1991), which includes algorithms for performing automatic object finding, star/galaxy classification, and total magnitude determination. Galaxy colors are measured using fixed apertures on the images of each filter, sampling identical regions of galaxies in different filters. Instrumental magnitudes are calibrated to the Kron-Cousins system by observing standard stars from Landolt (1992).

The 100% completeness limit of each field was set at 1.0 mag brighter than the magnitude of a stellar object with a brightness equivalent to having a  $S/N=5$  in an aperture of  $2''$  (see Yee 1991). Extinction values for each cluster are taken from the maps and tables of Burstein & Heiles (1982) and Burstein & Heiles (1984).

### 3. The Dwarf-to-Giant Ratio

In B07 we presented the composite cluster LF for the sample of 57 low-redshift clusters utilized in this paper. We found that, in general, the slope of the faint-end of the LF rises with increasing clustercentric radius. To further expand upon these findings, we have divided the cluster galaxy population into two sub-samples based on luminosity. Following the nomenclature used by previous studies (e.g., López-Cruz 1997; Driver et al. 1998; Popesso et al. 2006), we classify galaxies brighter than  $M_{R_c} = -20$  as “Giants” and those having  $-19.5 \leq M_{R_c} \leq -17.0$  as “Dwarfs”. We note that  $M_{R_c}^*$  calculated from these data (see B07) is  $M_{R_c}^* \sim -22.3$ . The measurement of  $R_c$ , including applied k-corrections, is described in B07. These magnitude cuts allow us to maximize the number of galaxies to improve statistical inferences while ensuring that incompleteness effects at the faint-end are negligible. We construct the cluster DGR by dividing the number of background-corrected dwarfs by the number of background-corrected giants. Only clusters 100% photometrically complete to  $M_{R_c} = -17$  are included in the construction of the DGR. Using this definition, we can employ the DGR to explore the change in the relative fraction of dwarfs and giants with respect to various cluster characteristics.

The primary advantage of using the DGR is that it provides a non-parametric measurement of the relative change in the number of giant and dwarf galaxies that is independent of the functional form selected for the cluster LF (e.g., a Schechter function; Schechter 1976).

For example, a steepening of the faint-end slope of the LF with increasing clustercentric radius would be characterized by an increase in the DGR (Driver et al. 1998). Given the degree of degeneracy between the parameters in a Schechter function fit (e.g.,  $M^*$  and  $\alpha$ ; B07), the DGR yields additional insights on the luminosity distribution of cluster galaxies and thus complements the LF.

### 3.1. DGR versus Richness

To examine for a possible correlation of the DGR with cluster richness, we plot in Figure 1 the DGR versus the richness parameter  $B_{gc}$  for 39 clusters that are 100% photometrically complete to  $M_{R_c} = -17.0$  (DGR uncertainties are calculated assuming Poisson statistics and quadrature summation). The cluster optical richness is parameterized by  $B_{gc}$ , which is a measure of the cluster center–galaxy correlation amplitude (Yee & López-Cruz 1999; Yee & Ellingson 2003; B07). In Figure 1 galaxies are selected within  $(r/r_{200}) = 0.4$  ( $\sim 900 h_{50}^{-1}$  kpc for the sample average) of each cluster center for the red+blue, red, and blue cluster galaxy populations. The red+blue cluster galaxy sample is compiled by including galaxies that have been culled of systems redder than the CMR for each individual cluster (for further details, see B07). The center of each cluster is chosen as the position of the brightest cluster galaxy (BCG) or, when some doubt exists, the nearest bright early-type galaxy to the X-ray centroid. The value of  $r_{200}$ , an approximate measure of the virial radius (Cole & Lacey 1996), is derived from the relationship between  $r_{200}$  and  $B_{gc}$  as described in B07 (see their equation 7), and is used as a scaling factor to minimize radial sampling bias due to variations in cluster richness (Christlein & Zabludoff 2003; Hansen et al. 2005; Popesso et al. 2006). The  $r_{200}$  measurements for our cluster sample are tabulated in Table 1 of B07 ( $r_{200}$  uncertainties are based on the 15% rms scatter in the derived value of  $r_{200}$  as explained in B07). The radial sampling criterion of  $(r/r_{200}) = 0.4$  was chosen to maximize the number of clusters in our sample that are photometrically complete to  $M_{R_c} = -17$ , and thus provide a large number of net galaxy counts to minimize the statistical uncertainty in the DGR.

Analysis of Figure 1 for the red+blue galaxies (top panel) indicates that there is no significant correlation between the DGR and cluster richness. A Kendell’s  $\tau$  statistic (Press et al. 1992) yields a 49% probability that the DGR and  $B_{gc}$  are correlated. When not employing a dynamical counting radius (e.g.  $r_{200}$ ), the mean and dispersion of the DGR vs.  $B_{gc}$  is increased significantly, indicating that the DGR is dependent on clustercentric radius (see §3.2 for further discussions).

We also plot in Figure 1 the DGR versus cluster richness for the red (middle panel) and

blue (bottom panel) galaxy populations. The color-selection of galaxies into red and blue samples is described in detail in B07. To briefly summarize; the red galaxies are chosen if they are located within  $\pm 0.22$  mag ( $3\sigma$ ) of the cluster CMR, while blue galaxies are selected from the area of the color-magnitude diagram that is blueward of the region used to select the red galaxies (see Figures 5 and 8 from B07). As noted for the combined red+blue galaxy population, the red and blue galaxies have been background-corrected using the exact same color-selection criteria as for the cluster galaxies.

Similar to the red+blue sample, we find no significant correlation between the DGR and richness when considering the red and blue galaxies separately. A Kendall’s  $\tau$  statistic indicates a 67% probability that the red DGR is correlated with  $B_{gc}$ ; while for the blue DGR, there is only a 3% probability that these quantities are correlated.

For the red+blue population we find a mean DGR of  $2.41_{-0.47}^{+1.28}$ , where the uncertainties bracket the interval containing 68% of the data points about the mean. For the red and blue samples we have  $1.30_{-0.38}^{+0.41}$  and  $11.20_{-4.61}^{+11.02}$ , respectively. The dominance of the dwarfs for the blue galaxy population compared to those in the red galaxy sample, is consistent with the findings from B07 in the sense that the blue LFs were found to have a steeper faint-end slope than the red sequence LFs. It is interesting to note that the blue DGR has a larger range of values and dispersion than the red DGR. This is an indication that blue galaxies in clusters have a larger variance in their properties and states of evolution compared to the red galaxies, which can be seen as primarily dominated by the end products of galaxy evolution and infall process.

### 3.2. DGR versus Clustercentric Radius

In B07 we presented evidence for a steepening of the LF faint-end slope towards the cluster outskirts. To investigate this correlation further, we plot in Figure 2 the DGR for the red+blue, red, and blue galaxy populations as a function of clustercentric radius. The DGR is plotted at the mid-point for the following annuli;  $(r/r_{200}) \leq 0.2$ ,  $0.2 \leq (r/r_{200}) \leq 0.4$ ,  $0.4 \leq (r/r_{200}) \leq 0.6$ , and  $0.6 \leq (r/r_{200}) \leq 1.0$ . The DGR is constructed by stacking cluster galaxies appropriate for each radial bin, and the uncertainty is derived from the standard deviation assuming Poisson statistics. Due to the variation in spatial imaging coverage, the number of clusters contributing to each radial bin is not equal. For all radius-dependent analysis in this study, we only include clusters that have complete spatial coverage for the indicated clustercentric radius.

Examination of Figure 2 shows that the DGR increases with radius for both the red and

red+blue galaxy populations. For the red+blue galaxy sample the DGR is 2.7 times larger for the outer-most annulus as compared to the inner-most radial bin ( $8.0\sigma$  difference). For the red galaxies the DGR is 2.0 times larger in the outer-most annulus as compared to the central region (significant at the  $4.3\sigma$  level). The DGR for the blue galaxies is approximately constant with perhaps even a possible decreasing trend with radius. We note that the uncertainties for the blue DGR are  $\sim 5$  times greater than those for the red and red+blue samples. This is a direct result of a small background-corrected blue giant count. A weighted linear least-squares fit to the blue galaxy data indicates that the radial slope of the DGR is different from zero at the  $1.7\sigma$  level. Although the error bars are relatively large, the distribution of the blue DGR suggests a mild rising trend with *decreasing* radius. The rise in the DGR with increasing radius for the red+blue galaxy sample is a reflection of the increasing dominance of blue galaxies with radius. This result is in agreement with Figures 4 and 7 from B07 where the red and red+blue galaxy populations were found to have a rising faint-end slope with increasing clustercentric radius. The faint-end slope of the blue galaxy LF depicted in Figure 10 from B07 indicates a much weaker dependence on radius.

Figure 2 also shows that for all radii depicted, the DGR is larger for the blue than for the red galaxy sample. This finding is also supported by the comparison of red and blue LFs presented in Figure 11 of B07, and is a result of the larger contribution of luminous galaxies to the red sample as compared to the blue population.

#### 4. The Blue Galaxy Fraction

A comparison of the number of red and blue galaxies gives a rough indication of the relative mixture of early- and late-type systems. Due to the poor seeing of our imaging data ( $\text{fwhm} \sim 1.5''$ ), morphological classification of galaxies with magnitudes near the completeness limit are not reliable. We therefore elect to use a broad-band color selection technique, such as the fraction of blue galaxies ( $f_b$ ; the number of blue galaxies divided by the number of red+blue galaxies), to glean some information about the galaxy population makeup of our sample. We note that  $f_b$  is constructed from background-corrected galaxy counts, and only includes clusters that are 100% photometrically complete for the indicated magnitude range.”

#### 4.1. Richness Dependence of $f_b$

In Figure 3 we present  $f_b$  versus cluster richness for galaxies selected within  $(r/r_{200}) = 0.8$  of each cluster center. To search for luminosity-related dependencies in the distribution of  $f_b$  with cluster richness, we plot  $f_b$  for galaxies with  $M_{R_c} \leq -17$  (14 clusters; open symbols) and  $M_{R_c} \leq -19$  (16 clusters; filled symbols). We note that the magnitude limit utilized by Butcher & Oemler (1984) to characterize the cluster blue fraction corresponds to  $M_{R_c} \sim -20.5$  using our adopted cosmology and filter (Fukugita et al. 1995). In order to minimize redshift bias (i.e., the dominance in our sample of rich clusters at high redshift), we selected a redshift range ( $z \leq 0.094$ ) such that a fair representation of cluster richness is available. Using clusters with  $z \leq 0.094$ , we find for the bright sample ( $M_{R_c} \leq -19$ ),  $\overline{f_b} = 0.23 \pm 0.08$ , while for the deep sample ( $M_{R_c} \leq -17$ ) we measure  $\overline{f_b} = 0.44 \pm 0.10$  (uncertainties are calculated assuming Poisson statistics). Examination of Figure 3 reveals that there is no significant correlation between  $f_b$  and  $B_{gc}$  for either the deep or bright sample. A Kendall's  $\tau$  statistic yields a 59%(47%) probability of a correlation for the deep(bright) sample. Using  $(r/r_{200}) = 1$  as our counting aperture also yields no significant correlation between  $f_b$  and  $B_{gc}$ . Using the equivalent Butcher & Oemler magnitude counting limit of  $M_{R_c} \sim -20.5$ , we find  $\overline{f_b} = 0.16 \pm 0.08$ . A Kendall's  $\tau$  statistic gives a 75% probability of a correlation between  $f_b$  and  $B_{gc}$ . Thus no significant correlation between  $f_b$  and cluster richness is discernible when counting galaxies within an equivalent dynamical radius. This indicates that the galaxy population in clusters is not dependent on cluster richness if a dynamics-dependent radius is used in sampling.

#### 4.2. Radial and Magnitude Dependence of $f_b$

To search for a possible radial dependence of  $f_b$ , we plot in Figure 4 the  $f_b$  in concentric annuli versus clustercentric radius for the dwarfs (open squares), giants (open triangles), and giants+dwarfs (filled circles) samples. Several aspects of the galaxy  $f_b$  are apparent: a) at any radius the dwarf galaxies have a greater  $f_b$  than the giants, b) the giant  $f_b$  increases approximately monotonically with increasing radius, with a five-fold increase from the inner to the outer radial bin ( $10\sigma$  difference), and c) the dwarf  $f_b$ , while decreasing by a factor of  $\sim 1.4$  at the inner-most radius, stays approximately constant at radii greater than  $(r/r_{200}) \sim 0.2$ .

To determine the relative change in the red and blue galaxies for the two inner-most radial bins, we restrict our cluster sample to include only those clusters that contribute to both annuli. Using this common cluster sample we find that there is a 53% decrease in the net number of blue dwarfs when comparing the  $0.2 \leq (r/r_{200}) \leq 0.4$  and  $(r/r_{200}) \leq 0.2$  radial



bins. On the other hand, the net number of red dwarfs decrease by 20%. For the giants we measure a decrease of 58% for the blue galaxies and a 7.1% *increase* for the red galaxies.

To ascertain the relative change in the radial-dependence of  $f_b$  as a function of magnitude, we present in Figure 5 the  $f_b$  as a function of  $M_{R_c}$  for the four radial bins used in Figure 4 ( $f_b$  is constructed by counting galaxies in bins of one magnitude in width). This figure demonstrates that  $f_b$  for the outer-most annulus ( $0.6 \leq (r/r_{200}) \leq 1.0$ ) is greater at each magnitude interval than for  $f_b$  measured for the inner annuli. In addition,  $f_b$  for all four radial bins generally show an increase when counting galaxies from progressively fainter magnitude bins. The data depicted in Figure 5 suggests that luminous galaxies may undergo a more rapid change in their color composition than the dwarf galaxies. For example,  $f_b$  for galaxies in the  $M_{R_c} = -22.5$  mag bin declines by a factor of 4.2 from the outer to the inner radial bin, while  $f_b$  decreases by a factor of 1.5 for galaxies in the  $M_{R_c} = -18.5$  mag bin ( $\sim 2.3\sigma$  difference in both cases).

As a caveat we note that our results based on Figures 4 and 5 demonstrate that the counting aperture and magnitude range has a direct impact on the value of  $f_b$ , and thus one must be cautious when comparing blue fractions for clusters with disparate masses from a variety of sources (see also, Ellingson et al. 2001; Fairley et al. 2002; De Propris et al. 2004; Popesso et al. 2007).

### 4.3. Redshift Dependence of $f_b$

To test for a correlation between  $f_b$  and redshift, we present in Figure 6 the  $f_b$  versus redshift for; a) galaxies brighter than  $M_{R_c} = -19$  (filled symbols; 54 clusters), b) galaxies selected with  $M_{R_c} \leq -17$  (open symbols; 39 clusters), and c) galaxies brighter than the equivalent Butcher & Oemler (1984) magnitude limit ( $M_{R_c} = -20.5$ ; solid triangles, 54 clusters). The  $f_b$ 's depicted in Figure 6 are constructed by including only galaxies within a clustercentric radius of  $(r/r_{200}) = 0.4$ . A Kendell's  $\tau$  statistic for the  $M_{R_c} \leq -19$  sample yields a probability of 100% that  $f_b$  and redshift are correlated. Inspection of Figure 6 shows that  $f_b$  increases with redshift for  $z \gtrsim 0.1$ . Restricting our analysis to clusters with  $z < 0.075$ , we find a correlation probability of only 8%. Thus most of the correlation between  $f_b$  and redshift is due to clusters with  $z \gtrsim 0.1$ . For the cluster sample with  $M_{R_c} \leq -17$ , we find that  $f_b$  and redshift are correlated at the 90% significance level. Limiting the  $M_{R_c} \leq -19$  sample to the same redshift range ( $z \leq 0.0865$ ), we find a correlation probability of 98%. Using the magnitude limit  $M_{R_c} = -20.5$  for the full redshift range ( $z < 0.2$ ), we find that  $f_b$  and redshift are correlated at the 97% significance level.

The correlation between  $f_b$  and redshift is most-likely a reflection of the Butcher-Oemler effect (Butcher & Oemler 1978, 1984), in which the fraction of blue cluster galaxies increases with look-back time. Since our cluster sample only extends to  $z \sim 0.2$ , we are not able to make any firm conclusions on the redshift evolution of  $f_b$ . However, Figure 6 and our correlation measurements indicate that the Butcher-Oemler effect is magnitude-dependent, such that a fainter magnitude limit yields a larger effect. Unfortunately our  $M_{R_c} \leq -17$  sample lacks a statistically significant number of clusters at  $z > 0.1$ .

## 5. Comparison with Other Results

### 5.1. Dynamical versus Fixed Clustercentric Radius

A major goal of this paper is to examine the luminosity and color distribution of individual and composite cluster galaxy populations. Many potential correlations may be obscured when only a limited number of cluster galaxies are available. To mitigate this effect, we compiled composite samples by stacking together galaxies from individual clusters. To minimize radial sampling bias, we scaled each cluster’s counting aperture by  $r_{200}$  prior to combining galaxy counts. Radial sampling bias can be problematic when comparing individual clusters (see, for example, B07), hence the need to scale clusters by a common dynamical radius. This point is aptly illustrated by the recent studies of Popesso et al. (2005, 2006) in which significant correlations between the DGR and various cluster characteristics (mass, velocity dispersion, X-ray luminosity, and optical luminosity) were found when measuring the DGR using a fixed metric aperture, but were much less significant when scaling the counting aperture by  $r_{200}$ . In a study by Margoniner et al. (2001) and Goto et al. (2003), cluster richness and  $f_b$  were found to be correlated such that poor systems have a higher  $f_b$ , which we suggest is the result of using a fixed counting aperture.

### 5.2. Dependence on Magnitude Limits

Our results, along with those from many others, show that quantities such as the DGR and  $f_b$  are dependent on the luminosity definitions of the galaxy samples used. When comparing different studies, care should be taken to account for any possible effects arising from the galaxy luminosity or mass limits. Some recent studies have examined the DGR and  $f_b$  based on spectroscopic data from the SDSS galaxy sample (e.g., Aguerri et al. 2007; Popesso et al. 2007; Sánchez-Janssen et al. 2008). However, these studies, while statistically more robust, are in general much shallower than investigations applying a statistical

background correction method to photometric data. Studies using photometric galaxy samples, going typically two to three magnitudes deeper, provide considerably larger leverage in sampling the dependence of galaxy population and evolution on luminosity/mass.

### 5.3. Dwarf-to-Giant Ratio

In a study by De Propris et al. (2003) the DGR for a spectroscopically-measured sample of 60 clusters from the 2dF Galaxy Redshift Survey were presented. Transforming their magnitudes to  $R_C$  (Fukugita et al. 1995) and adopting our cosmology, De Propris et al. defines giants as those galaxies with  $-24.4 \leq M_{R_c} \leq -20.9$  and dwarfs with  $-20.9 \leq M_{R_c} \leq -18.9$ . They divide their galaxies based on spectroscopic type, and find  $\text{DGR} = 1.29 \pm 0.16$  and  $4.88 \pm 0.97$  for galaxies with early- and late-type spectra, corresponding to our red and blue galaxy samples. Their results show the same trend as ours for red and blue galaxies (§3.1). The blue DGR obtained by De Propris et al. is smaller than the value we measured, and is likely due to their division between the giant and dwarf populations being almost 2 mag brighter.

We also note that De Propris et al. counts galaxies within an aperture of  $3h_{50}^{-1}$  Mpc in radius rather than scaling relative to a dynamical radius. They also determined that the DGR is smaller for galaxies selected within  $0.6h_{50}^{-1}$  Mpc of the composite cluster center as compared to galaxies at larger radii ( $2.2\sigma$  difference). In Figure 2 we showed that the DGR increases with clustercentric radius for the red+blue cluster galaxy population (at the  $8\sigma$  level). We suggest that the De Propris et al. result would be of higher significance if the cluster counting aperture was scaled by a common dynamical radius.

In addition, De Propris et al. reports no statistically significant correlation ( $\lesssim 1\sigma$ ) between cluster velocity dispersion (divided at  $\sigma = 800 \text{ km s}^{-1}$ ) and the DGR, or between “rich” and “poor” clusters. This result is consistent with our data depicted in Figure 1, even though we sample 2 mag deeper than De Propris et al. and scale by  $r_{200}$ .

From a study of 69 clusters selected from the RASS-SDSS catalog, Popesso et al. (2006) presented the DGR for various cluster galaxy sub-samples. Using  $r_{200}$  as a scaling factor, Popesso et al. found that the DGR is not correlated with cluster mass (i.e.,  $M_{200}$ ), velocity dispersion, or  $L_X$ . This result is compatible with our findings depicted in Figure 1, where we find no significant correlation between the DGR and  $B_{gc}$  for the red+blue, red, and blue galaxy populations. Using the  $L_X$  (0.1-2.4 keV) measurements compiled by Ebeling et al. (1996, 2000), we examined the DGR vs.  $L_X$  distribution for galaxies selected within  $(r/r_{200}) \leq 0.4$ . Applying the Kendell’s  $\tau$  statistic to the red+blue/red/blue galaxy

samples, we find a 87%/91%/29% probability that the DGR and  $L_X$  are correlated. Our findings support the results of Popesso et al. in that there is no strong, statistically significant correlation between the DGR and  $L_X$ .

#### 5.4. Blue Galaxy Fraction

In addition to examining the DGR for the composite cluster galaxy population, Popesso et al. divided their sample into red and blue galaxies by adopting  $u - r = 2.22$  as the dividing color threshold. Popesso et al. found that the fraction of red and blue dwarf galaxies decreases toward the cluster center (see their Figure 12a). Although they plot the cumulative fractional change in the number of dwarfs, it is apparent that Popesso et al. detects a more statistically significant drop in the fraction of blue dwarf galaxies than what we find (see Figure 2). This difference may be related to their utilization of the  $u$ -band for the selection of blue galaxies and differences in the magnitude range used to define giants and dwarfs.

In Figure 12b from Popesso et al., the dwarf red-to-blue ratio (RBR) is depicted as a function of clustercentric radius, normalized to  $r_{200}$ . This figure shows that the RBR is approximately constant from  $0.4 < (r/r_{200}) < 1.0$  ( $\text{RBR} \sim 0.6$ ) and increases to  $\sim 2.4$  near the cluster center. Comparison with our Figure 4 shows that our  $f_b$  is consistent with this result. Computing RBR for our dwarf sample yields  $\text{RBR} \sim 0.6$  for  $(r/r_{200}) > 0.4$  and  $\sim 1.4$  for the inner-most annulus. These values are similar to those found by Popesso et al. given their smaller radial bins.

In a recent study, Aguerri et al. (2007) presented the blue galaxy fraction for a sample of 88 clusters ( $z < 0.1$ ) selected from the SDSS-DR4 data set. The blue galaxy fraction was constructed by including galaxies brighter than  $M_r = -20$  and located within a radius of  $(r/r_{200}) = 1$ . Aguerri et al. found that  $f_b$  is correlated with  $L_X$  in the sense that low  $f_b$  clusters have a greater  $L_X$  ( $3\sigma$  difference). This result is also supported by Popesso et al. (2007), who measured  $f_b$  for a sample of 79 clusters from the RASS-SDSS cluster catalog by including spectroscopically-detected galaxies within  $(r/r_{200}) = 1$ .

Using X-ray data from Ebeling et al., we find that  $f_b$  and  $L_X$  are not significantly correlated. For galaxies brighter than  $M_{R_c} = -17$  and located within  $(r/r_{200}) = 0.4$ , a Kendall's  $\tau$  statistic yields a 17% probability of a correlation. Restricting our analysis to  $M_{R_c} \leq -19$ , we find a 65% probability of a correlation. Transforming the magnitude limit utilized by Aguerri et al. to our filter and distance scale ( $M_{R_c} \sim -21$ ), we find a 80% probability of a correlation. Our results are in agreement with Fairley et al. (2002) and

Wake et al. (2005), who found no significant correlation between  $f_b$  and  $L_X$ .

Utilizing a sample of 60 clusters ( $z < 0.11$ ) selected spectroscopically from the 2dFGRS, De Propris et al. (2004) searched for correlations between  $f_b$  and various cluster properties. In Figure 5 we showed that  $f_b$  is sensitive both to the adopted absolute magnitude range and clustercentric distance used to select galaxies. De Propris et al. reached a similar conclusion by determining that  $f_b$  increases both with decreasing luminosity and increasing clustercentric radius. In addition, De Propris et al. also found that there is no significant correlation between  $f_b$  and cluster richness when measured within  $(r/r_{200}) = 0.5$ . This is also in agreement with our results depicted in Figure 3.

## 6. Discussion

In this study we have examined the radial dependence of the luminosity and color distribution of cluster galaxies by utilizing the DGR and  $f_b$ . Scaling the galaxy counting aperture relative to  $r_{200}$ , allows us to minimize radial sampling bias.

The main results highlighted in this paper and encapsulated in Figures 2 and 4, suggests that some type of dynamical mechanism may be responsible for the decline in the number of blue dwarf galaxies relative to the corresponding red systems in the cluster core region. The trend depicted in Figure 2 implies that the DGR for the blue galaxies is approximately constant with radius. This suggests that the decrease in the number of blue dwarfs toward the cluster center is accompanied by a decline in the number of blue giants, thus maintaining a roughly constant DGR. A decrease in  $f_b$  for the giant galaxies in the cluster core region (Figure 4) and a drop in the DGR for the red galaxies, suggests that the relative fraction of red giants increases toward the cluster center.

These results support the general view that blue galaxies dominate the galaxy population in the outskirts of clusters in contrast to the central cluster region (e.g., Ellingson et al. 2001; Fairley et al. 2002; Dahlnén et al. 2004; Tran et al. 2005). They also imply that field galaxies, which are generally bluer than cluster galaxies (see, for example, Lewis et al. 2002; McIntosh et al. 2004), fall into the cluster environment, turn red (possibly via some process that truncates star formation), and that blue dwarf galaxies get preferentially disrupted or transformed into red dwarfs at small clustercentric radii.

### 6.1. Possible Interpretations

These findings are open to several possible interpretations: a) blue and red dwarfs get disrupted tidally or undergo mergers with giant galaxies at roughly the same rate, which destroy individual dwarfs, except in the cluster core region, where the red dwarfs have a higher survival rate; b) the average dwarf galaxy star formation rate remains relatively unchanged until the dwarfs reach the central cluster region, where the influence of ram pressure and cluster tidal effects are expected to be maximized (e.g., Moore et al. 1996), quenching star formation and transforming the galaxies into red dwarfs; and c) the transformation rate of blue into red galaxies resulting from the quenching of star formation is more efficient in giants than in dwarfs (see Figure 5).

The first interpretation requires that blue dwarfs are more susceptible than red dwarfs to destructive forces in the cluster central region. Some support for this idea is garnered from the fact that blue dwarfs are very similar to the low-mass dwarf spheroidal galaxies, which are expected to undergo tidal disruption in the cluster environment (Thompson & Gregory 1993; Gallagher & Wyse 1994; Moore et al. 1999; Quilis et al. 2000; Boyce et al. 2001; Barai et al. 2007). These galaxies may potentially be the source of tidally-disrupted material that helped to form the halo of cD galaxies (López-Cruz et al. 1997b; Hilker et al. 1999, 2003). The red dwarf galaxies, however, may be part of a population of nucleated dwarfs (van den Bergh 1986; Caldwell & Bothun 1987; Lisker et al. 2007) that would be expected to have a deeper gravitational potential well than the more diffuse dwarf spheroidal population. This would allow them to more efficiently survive cluster tidal forces against disruption than the dwarf spheroidals (i.e., non-nucleated dwarf galaxies; see, for example, Thompson & Gregory 1993; Trujillo et al. 2002; Barai et al. 2007; Lisker et al. 2007). Nucleated cluster dwarf galaxies have been shown to have colors that are redder on average than non-nucleated dwarfs (e.g. Caldwell & Bothun 1987; Lisker et al. 2007), and thus supports the suggestion that the red dwarf population is composed mainly of nucleated dwarf galaxies.

For the second scenario, if the blue dwarf galaxies in the cluster core have been stripped of their gas, had their star formation truncated, and transformed into red dwarf galaxies, we would expect that the number of red dwarf galaxies would increase with decreasing clustercentric radius. Figure 2 indicates that the red DGR actually decreases by a factor of  $\sim 2$  toward the inner-cluster region. Unless a large fraction of blue giants, as compared to blue dwarfs, get transformed into red systems, this simple explanation for the decreasing number of blue dwarfs in the core does not seem plausible. Furthermore, Figure 2 indicates that the blue DGR is approximately constant with radius, contrary to what is expected if a large fraction of blue giants are transformed into red galaxies in order to decrease the red DGR in the cluster core.

The third explanation supposes that the quenching of star formation is more efficient in giant galaxies than in dwarfs. Naively, this conjecture can be supported from the results in Figure 5, where the more luminous galaxies show a larger decrease in  $f_b$  from the outer- to the inner-cluster region than the less luminous galaxy population. However, this seems an unlikely explanation, since, with their lower gravitational potential, we would expect most physical mechanisms in clusters that affects star formation rate in galaxies should have a relatively larger effect in dwarf galaxies than the more massive giant galaxies.

## 6.2. Galaxy Disruption versus Fading

The tidal disruption of dwarf galaxies is a possible physical mechanism to help explain the observations presented in this paper; an alternative interpretation is that the blue dwarf galaxies simply fade and turn red as they fall toward the cluster center, and are subsequently detected as red galaxies in the inner-cluster region. This idea is not unreasonable if we expect that star formation for infalling dwarf galaxies gets truncated, with an ensuing passive evolution of the stellar population (e.g., Abraham et al. 1996; Ellingson et al. 2001; Treu et al. 2003; Smith et al. 2006).

The exact number of blue dwarfs that would be expected to fade and turn red, or to disappear due to disruption or merger, cannot be accurately calculated with a simple toy model. A detailed N-body simulation that incorporates a complete accounting of stellar evolution and traces the evolutionary path of each dwarf galaxy would be required. Nevertheless, we are able to place limits on the fraction of blue dwarfs that have faded and turned red or that have been disrupted, by comparing the blue-to-red dwarf luminosity ratio between the inner- ( $L_b^i/L_r^i$ ) and outer-most ( $L_b^o/L_r^o$ ) radial bins.

For the case of pure disruption,  $L_b^o/L_r^o$  was measured for the  $0.6 \leq (r/r_{200}) \leq 1.0$  radial bin using background-corrected net galaxy counts. The luminosity of the blue and red galaxies were calculated by multiplying the number of galaxies per magnitude bin with the luminosity-equivalent of the mid-bin magnitude. Using our magnitude definition of a dwarf galaxy (i.e.,  $-19.5 \leq M_{R_c} \leq -17.0$ ), we find that  $L_b^o/L_r^o = 1.81$ .

For the inner annulus,  $(r/r_{200}) \leq 0.2$ ,  $L_b^i/L_r^i$  was calculated in the same manner as for the outer radial bin except that the magnitude distribution of the background-corrected galaxies is determined using the deprojected cluster LF (see B07). The deprojected LF is constructed by subtracting the contribution of galaxies located in the cluster outskirts that are projected onto the central cluster region. The deprojected LF thus provides a more accurate estimate of the galaxy luminosity distribution in the cluster center, especially at

the faint end. Using the deprojected LF, we found that  $L_b^i/L_r^i = 0.34$ . Using our measured luminosity ratios, the expected fraction of disrupted blue dwarfs ( $f$ ) can be estimated from  $L_b^i/L_r^i = (1 - f)(L_b^o/L_r^o)$ . Solving for  $f$  we find  $f = 0.81$ , and thus approximately 81% of the blue dwarfs would undergo disruption as they fall into the central cluster region.

For the case of pure fading with an associated reddening, we employ the library of evolutionary stellar population synthesis models computed using the isochrone code of Bruzual & Charlot (2003), to provide an estimate of the amount of fading/reddening that an infalling galaxy would experience. Adopting the concordance cosmological parameters (i.e.,  $\Omega_m = 0.3$ ,  $\Omega_\lambda = 0.7$ , and  $H_0 = 70 h_{70} \text{ km s}^{-1} \text{ Mpc}^{-1}$ ), the timescale for the infall of a typical dwarf galaxy from the  $0.6 \leq (r/r_{200}) \leq 1.0$  annulus is estimated by adopting the average value of  $r_{200}$  and the mean velocity dispersion for our 57-cluster sample. Using the  $B_{gc}$  values tabulated in B07, and the relationship between  $B_{gc}$  and velocity dispersion from Yee & Ellingson (2003), we find  $\overline{r_{200}} = 1.6 h_{70}^{-1} \text{ Mpc}$  and  $\overline{\sigma_v} = 840 \text{ km s}^{-1}$ . Using these values yields an average infall timescale of approximately 2 Gyr. Adopting a Salpeter Initial Mass Function (Salpeter 1955), solar metallicity, a single-burst star formation model to simulate star formation truncation, and a 2 Gyr time-frame for passive evolution, we predict a  $\sim 0.2$  mag fading in  $R_C$  and a reddening of  $\Delta(B - R_c) \sim 0.5$  mag.

For the case of fading/reddening of dwarf galaxies, we invoke a similar procedure as that used for the disruption scenario. For this case we count dwarf galaxies in the  $0.6 \leq (r/r_{200}) \leq 1.0$  annulus using the magnitude range  $-19.7 \leq M_{R_C} \leq -17.2$  in order to compensate, to first order, for the expected 0.2 mag fading for an infalling galaxy. For the outer radial bin we find  $L_b^o/L_r^o = 1.46$ . The expected fraction of galaxies that have undergone fading with an associated reddening can be estimated from  $L_b^i/L_r^i = (1 - f)L_b^o/(L_r^o + fL_b^o)$ . Solving for  $f$  yields  $f = 0.57$ , and thus approximately 57% of the blue dwarfs would be expected to have undergone fading and reddening as they reach the inner-cluster region.

It seems unlikely, however, that a pure fading scenario can explain the change of  $f_b$  seen from the outer to inner region of clusters. First, applying the same procedure of fading to the giant galaxies, we find that 80% of the blue galaxies are expected to undergo fading and reddening by the time they reach the cluster core from the outer annulus. This is likely the dominant cause for the change in  $f_b$  for the giant galaxies, since it is unlikely that they can be easily destroyed by tidal forces. If we assume that blue dwarfs were to fade by the same fraction, then the dwarf blue-to-red luminosity would be much smaller than what is measured, by a factor of about  $\sim 2.5$ ; unless some mechanism is invoked that fades blue giant galaxies by a much larger fraction than dwarf galaxies. Due to the lower gravitational potential possessed by dwarf galaxies, almost all mechanisms used to explain the hastening of galaxy evolution in rich environments operate equally or more efficiently for lower-mass



galaxies; e.g., ram pressure, tidal interactions, harassment, etc. The only mechanism that could produce a higher fraction of the quenching of star formation in massive galaxies is AGN feedback, in that more massive galaxies will be more likely to contain a massive black hole required for the AGN activity.

Second, in a pure fading scenario for dwarf galaxies, we would expect the DGR for the blue+red sample to stay approximately constant from the outer to the inner region, unless the parent populations of galaxies from which the inner and outer regions are drawn from are very different. Instead, we find there is a factor of 4 difference in the DGR between the outer annulus and the cluster core.

While the discussion above cannot completely rule out the pure fading scenario, it seems likely that, as blue dwarf galaxies fall into the cluster core, at least some fraction of them will be destroyed either by tidal disruption, or mergers with larger galaxies.

## 7. Conclusions

In this paper we have studied the luminosity and color properties of a sample of 57 low-redshift Abell clusters. Our main conclusions are:

1) The DGR for the red, blue, and red+blue cluster galaxies are independent of cluster richness when scaling the counting aperture by a dynamical radius (i.e.,  $r_{200}$ ). Also, the DGR for blue galaxies is larger than for red systems.

2) The DGR for the red galaxies decreases in the inner cluster region, while the blue DGR is approximately constant as a function of cluster-centric radius.

3) The  $f_b$  was found not to correlate with cluster richness when counting galaxies within a dynamical radius; however, it is found to be correlated with the adopted counting aperture and magnitude limit.

4) The  $f_b$  for dwarf galaxies was found to be approximately constant with clustercentric radius except in the cluster core region where  $f_b$  decreases.

5) The  $f_b$  for giant galaxies was found to increase with clustercentric radius for all measured annuli.

6) Based on the clustercentric radial dependence of the DGR and the galaxy blue fraction, it is unlikely that either a pure disruption or a pure fading/reddening scenario can describe the evolution of infalling dwarf galaxies; both outcomes are produced by the cluster environment.

We thank the anonymous referee for reviewing our paper. Research by W. A. B. is supported by a start-up grant from the University of North Dakota. Research by H. K. C. Y. is supported by an NSERC Discovery grant. O. L.-C research is supported by INAOE and a CONACyT grant for Ciencia Básica P45952-F. O. L.-C. acknowledges support from a research grant from the Academia Mexicana de Ciencias-Royal Society during 2006-2007 taken to the University of Bristol. OLC acknowledges Gus Oemler for suggesting the use of non-parametric DGR. We thank Huan Lin for providing photometric catalogs for five control fields, and James Brown for the use of his galaxy profile fitting software and photometric data for A496 and A1142.

The Image Reduction and Analysis Facility (IRAF) is distributed by the National Optical Astronomy Observatory, which is operated by AURA, Inc., under contract to the National Science Foundation. This research has made use of the NASA/IPAC Extragalactic Database (NED) which is operated by the Jet Propulsion Laboratory, California Institute of Technology, under contract with the National Aeronautics and Space Administration.

## REFERENCES

- Abadi, M. G., Moore, B., & Bower, R. G. 1999, *MNRAS*, 308, 947
- Abraham, R. G., et al. 1996, *ApJ*, 461, 694
- Aguerri, J. A. L., Sánchez-Janssen, R., & Muñoz-Tuñón, C. 2007, *A&A*, 471, 17
- Barai, P., Brito, W., & Martel, H. 2007, preprint (astro-ph/0707.1533)
- Barkhouse, W. A. 2003, Ph.D. Thesis, Univ. Toronto
- Barkhouse, W. A., Yee, H. K. C., & López-Cruz, O. 2007, *ApJ*, 671, 1471
- Boselli, A., & Gavazzi, G. 2006, *PASP*, 118, 517
- Boyce, P. J., Phillipps, S., Jones, J. B., Driver, S. P., Smith, R. M., & Couch, W. J. 2001, *MNRAS*, 328, 277
- Brown, J. P. 1997, Ph.D. thesis, Univ. Toronto
- Bruzual, G., & Charlot, S. 2003, *MNRAS*, 344, 1000
- Burstein, D., & Heiles, C. 1982, *AJ*, 87, 1165
- Burstein, D., & Heiles, C. 1984, *ApJS*, 54, 33
- Butcher, H., & Oemler, A. 1978, *ApJ*, 219, 18
- Butcher, H., & Oemler, A. 1984, *ApJ*, 285, 426
- Caldwell, N., & Bothun, G. D. 1987, *AJ*, 94, 1126
- Christlein, D., & Zabludoff, A. I. 2003, *ApJ*, 591, 764
- Cole, S., & Lacey, C. 1996, *MNRAS*, 281, 716
- Dahlén, T., Fransson, C., Östlin, G., & Näslund, M. 2004, *MNRAS*, 350, 253
- De Propriis, R., et al. 2003, *MNRAS*, 342, 725
- De Propriis, R., et al. 2004, *MNRAS*, 351, 125
- Dressler, A. 1980, *ApJ*, 236, 351
- Dressler, A., et al. 1997, *ApJ*, 490, 577

- Driver, S. P., Couch, W. J., & Phillipps, S. 1998, MNRAS, 301, 369
- Dubinski, J. 1998, ApJ, 502, 141
- Ebeling, H., Voges, W., Böhringer, H., Edges, A. C., Huchra, J. P., & Briel, U. G. 1996, MNRAS, 281, 799
- Ebeling, H., Edges, A. C., Allen, S. W., Crawford, C. S., Fabian, A. C., & Huchra, J. P. 2000, MNRAS, 318, 333
- Ellingson, E., Lin, H., Yee, H. K. C., & Carlberg, R. G. 2001, ApJ, 547, 609
- Fairley, B. W., Jones, L. R., Wake, D. A., Collins, C. A., Burke, D. J., Nichol, R. C., & Romer, A. K. 2002, MNRAS, 330, 755
- Fukugita, M., Shimasaku, K., & Ichikawa, T. 1995, PASP, 107, 945
- Gallagher, J. S., & Wyse, R. F. G. 1994, PASP, 106, 1225
- Goto, T., et al. 2003, PASJ, 55, 739
- Hansen, S. M., McKay, T. A., Wechsler, R. H., Annis, J., Sheldon, E. S., & Kimball, A. 2005, ApJ, 633, 122
- Hilker, M., Infante, L., & Richtler, T. 1999, A&AS, 138, 55
- Hilker, M., Mieske, S., & Infante, L. 2003, A&A, 397, L9
- Jones, C., & Forman, W. 1999, ApJ, 511, 65
- Kent, S. M., & Gunn, J. E. 1982, AJ, 87, 945
- Landolt, A. U. 1992, AJ, 104, 372
- Lewis, I., et al. 2002, MNRAS, 334, 673
- Lisker, T., Grebel, E. K., Binggeli, B., & Glatt, K. 2007, ApJ, 660, 1186
- López-Cruz O. 1997, Ph.D. Thesis, Univ. Toronto
- López-Cruz, O., Yee, H. K. C., Brown, J. P., Jones, C., & Forman, W. 1997, ApJ, 475, L97
- López-Cruz, O. 2001, Rev. Mex. Astron. Astrophys, Conf. Ser., 11, 183
- López-Cruz, O., Barkhouse, W. A., & Yee, H. C. K. 2004, ApJ, 614, 679

- Margoniner, V. E., De Carvalho, R. R., Gal, R. R., & Djorgovski, S. G. 2001, *ApJ*, 548, L143
- McIntosh, D. H., Rix, H.-W. & Caldwell, N. 2004, *ApJ*, 610, 161
- Merritt, D. 1984, *ApJ*, 276, 26
- Moore, B., Katz, N., Lake, G., Dressler, A., & Oemler, A. 1996, *Nature*, 379, 613
- Moore, B., Lake, G., Quinn, T., Stadel, J. 1999, *MNRAS*, 304, 465
- Morris, S. L., Hutchings, J. B., Carlberg, R. G., Yee, H. K. C., Ellingson, E., Balogh, M. L., Abraham, R. G., & Smecker-Hane, T. A. 1998, *ApJ*, 507, 84
- Okamoto, T., & Nagashima, M. 2001, *ApJ*, 547, 109
- Popesso, P., Böhringer, H., Romaniello, M., & Voges, W. 2005, *A&A*, 433, 415
- Popesso, P., Biviano, A., Böhringer, H., & Romaniello, M. 2006, *A&A*, 445, 29
- Popesso, P., Biviano, A., Romaniello, M., & Böhringer, H. 2007, *A&A*, 461, 411
- Press, W. H., Teukolsky, S. A., Vetterling, W. T., & Flannery, B. P. 1992, *Numerical Recipes, The Art of Scientific Computing*, (2d ed.; Cambridge: Cambridge University Press)
- Quilis, V., Moore, B., & Bower, R. 2000, *Science*, 288, 1617
- Rood, H. J., Page, T. L., Kintner, E. C., & King, I. R. 1972, *ApJ*, 175, 627
- Roos, N., & Norman, C. A. 1979, *A&A*, 76, 75
- Salpeter, E. E. 1955, *ApJ*, 121, 161
- Sánchez-Janssen, R., Aguerri, J. A. L., & Muñoz-Tuñón, C. 2008, *ApJ*, 679, L77
- Schechter, P. 1976, *ApJ*, 203, 297
- Smith, R. J., Hudson, M. J., Lucey, J. R., Nelan, J. E., & Wegner, G. A. 2006, *MNRAS*, 369, 1419
- Thomas, T., & Katgert, P. 2006, *A&A*, 446, 31
- Thompson, L. A., & Gregory, S. A. 1993, *AJ*, 106, 2197
- Thuan, T. X., & Gunn, J. E. 1976, *PASP*, 88, 543

- Tran, K.-V. H., van Dokkum, P., Illingworth, G. D., Kelson, D., Gonzalez, A., & Franx, M. 2005, *ApJ*, 619, 134
- Treu, T., Ellis, R. S., Kneib, J.-P., Dressler, A., Smail, I., Czoske, O., Oemler, A., & Natarajan, P. 2003, *ApJ*, 591, 53
- Trujillo, I., Aguerri, J. A. L., Gutiérrez, C. M., Caon, N., & Cepa, J. 2002, *ApJ*, 573, 9
- van den Bergh, S. 1986, *AJ*, 91, 271
- Wake, D. A., Collins, C. A., Nichol, R. C., Jones, L. R., & Burke, D. J. 2005, *ApJ*, 627, 186
- Wolf, C., Gray, M. E., Aragón-Salamanca, A., Lane, K. P., & Meisenheimer, K. 2007, *MNRAS*, 376, L1
- Yee, H. K. C. 1991, *PASP*, 103, 396
- Yee, H. K. C., & López-Cruz, O. 1999, *AJ*, 117, 1985
- Yee, H. K. C. & Ellingson, E. 2003, *ApJ*, 585, 215

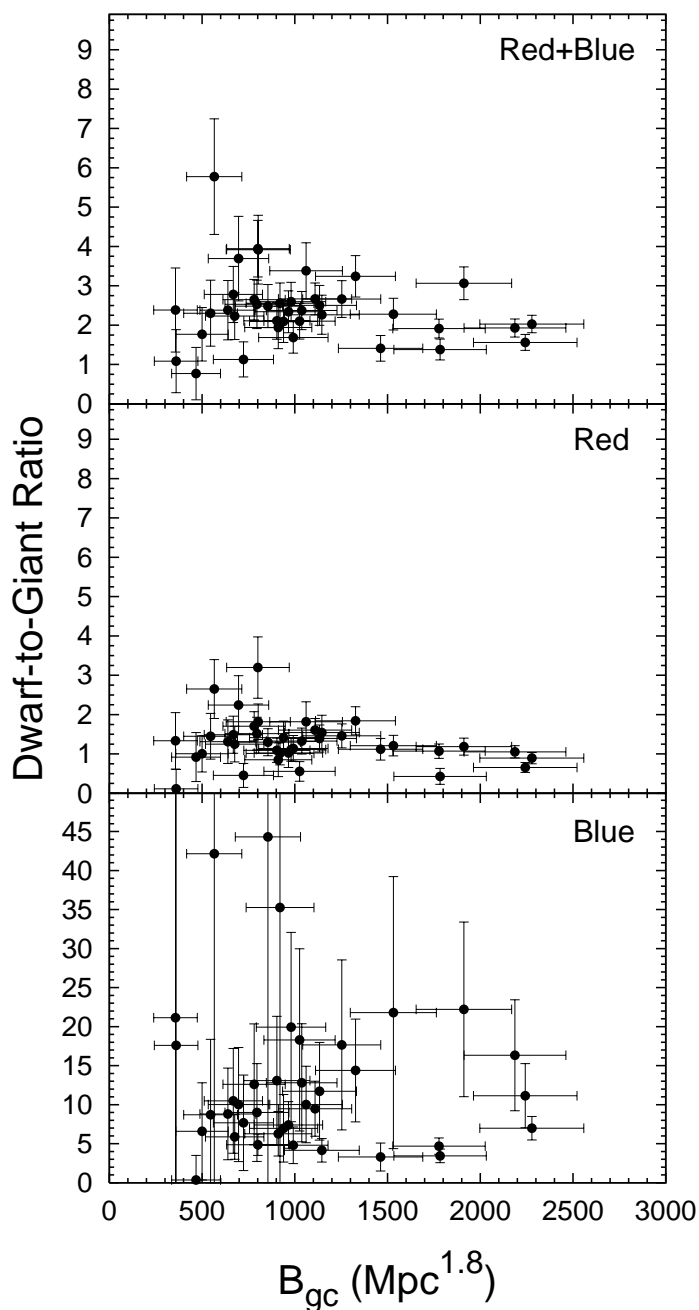


Fig. 1.— Comparison of the DGR with cluster richness for the red+blue (*top*), red (*middle*), and blue (*bottom*) galaxy populations that are photometrically complete to  $M_{R_c} = -17$ . The DGR is calculated for galaxies measured within  $(r/r_{200}) \leq 0.4$ .

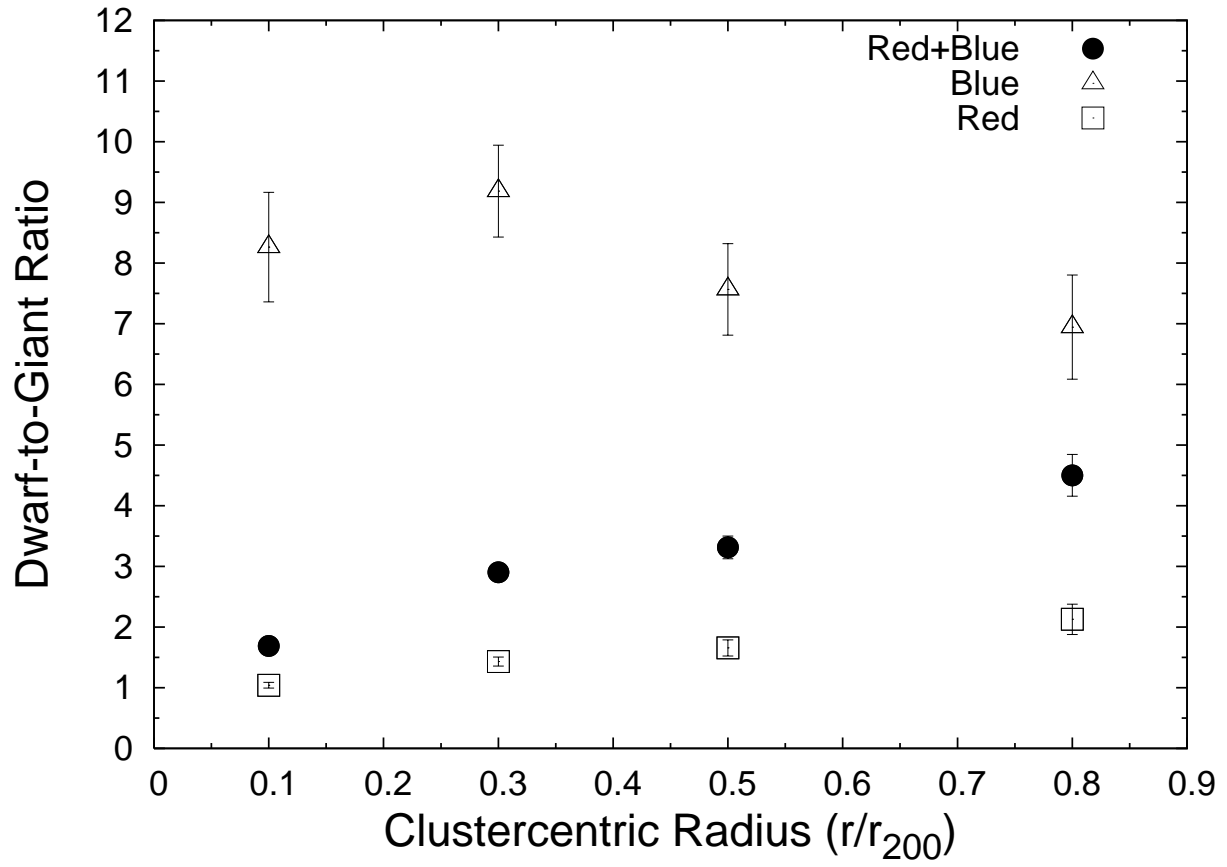


Fig. 2.— DGR as a function of clustercentric radius for the red+blue (filled circles), red (open squares), and blue (open triangles) cluster galaxy populations.



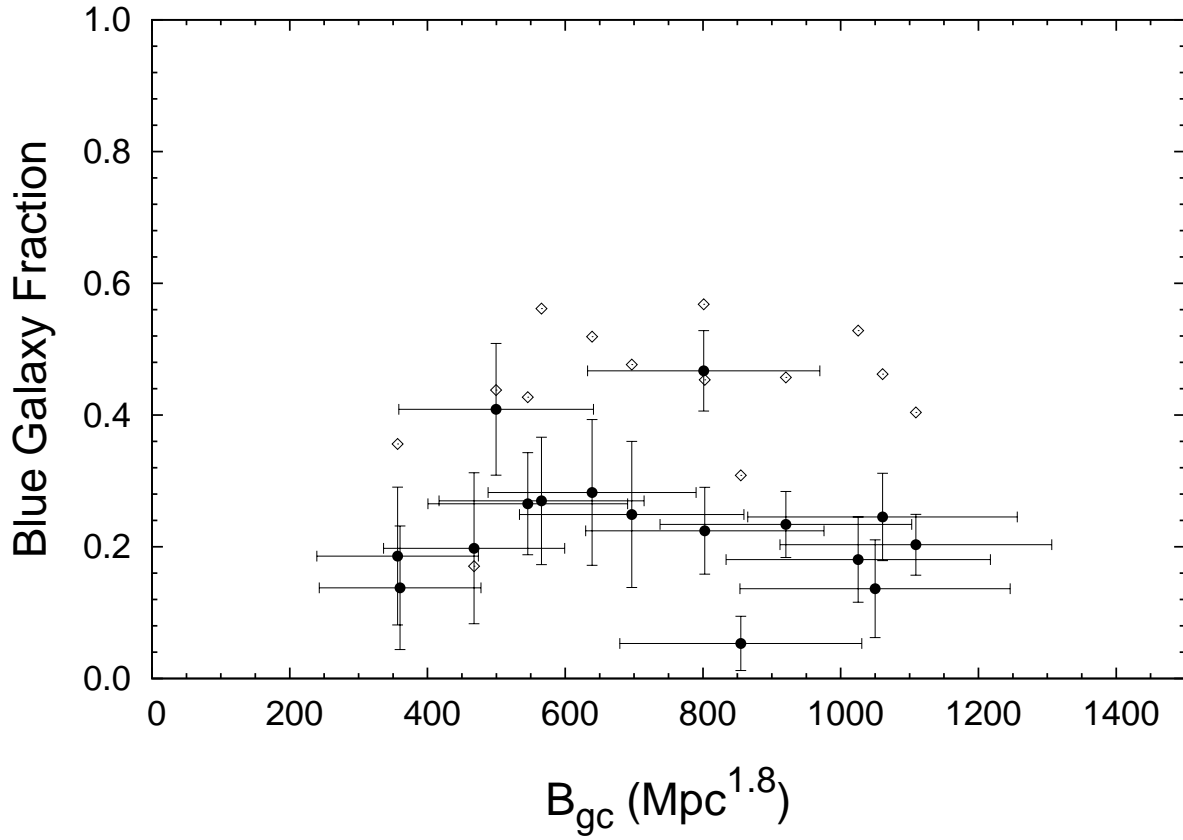


Fig. 3.—  $f_b$  as a function of cluster richness ( $B_{gc}$ ) for the cluster galaxy population complete to  $M_{R_c} = -19$  (filled circles) and  $M_{R_c} = -17$  (open diamonds). Error bars for the open symbols are similar to the filled circles and have been omitted for clarity. Galaxies have been measured within a clustercentric radius of  $(r/r_{200}) = 0.8$ .

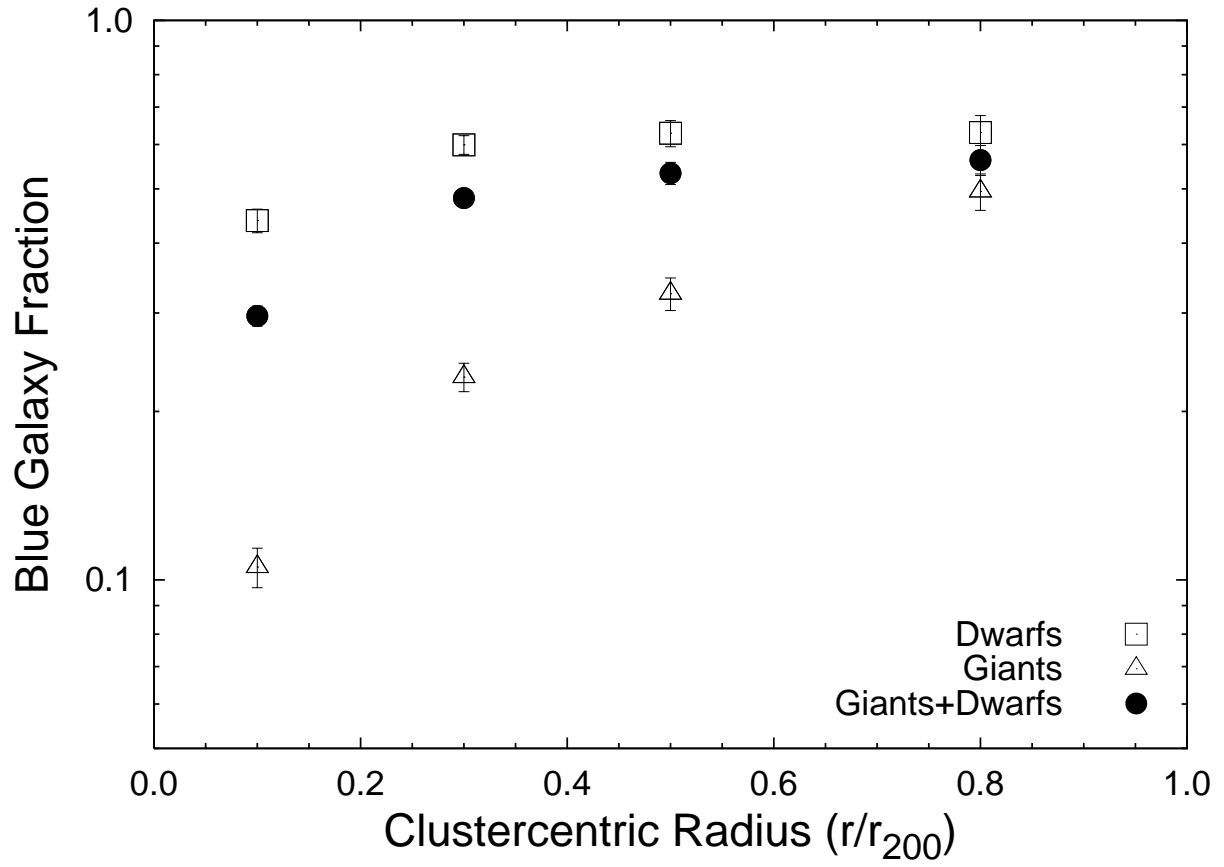


Fig. 4.—  $f_b$  as a function of clustercentric radius for the giants (open triangles), dwarfs (open squares), and giants+dwarfs (filled circles) cluster galaxy populations.

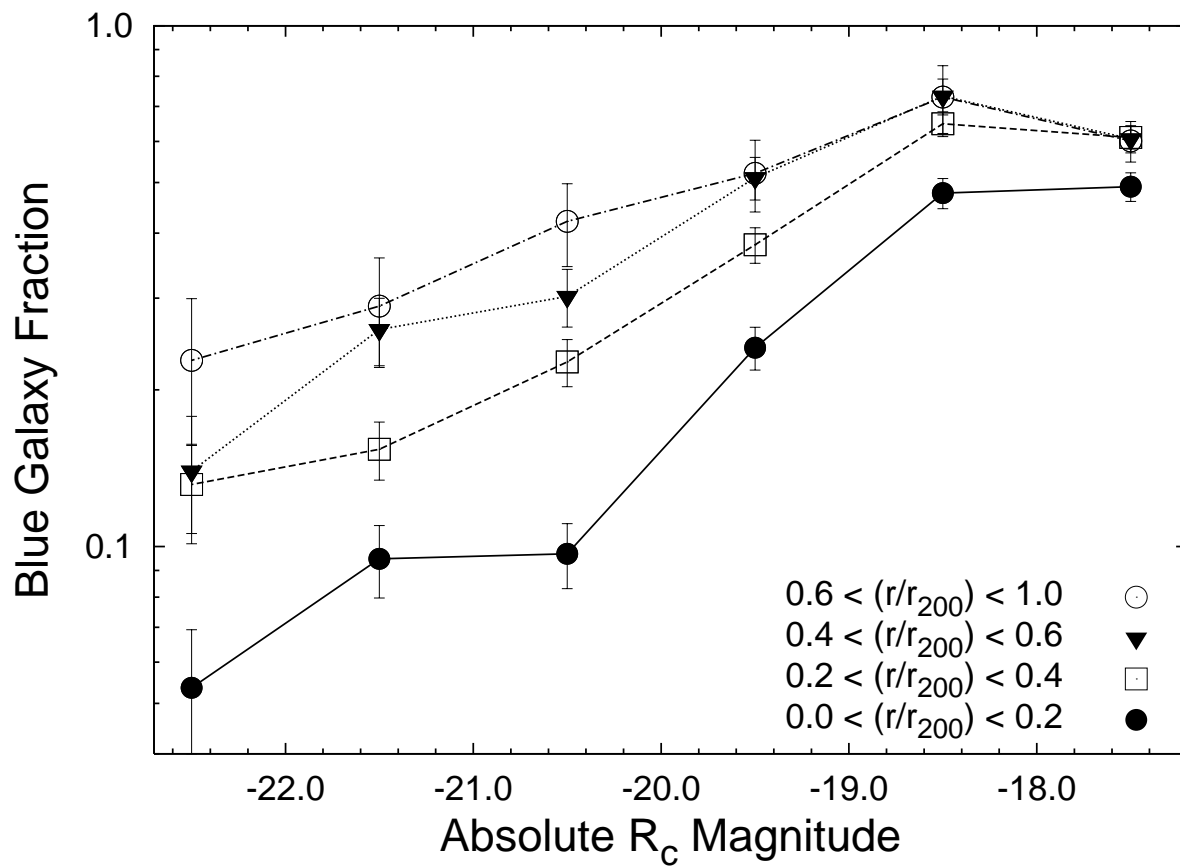


Fig. 5.—  $f_b$  as a function of magnitude ( $M_{R_c}$ ) for four radial bins;  $(r/r_{200}) \leq 0.2$  (filled circles with solid line),  $0.2 < (r/r_{200}) < 0.4$  (open squares with dashed line),  $0.4 < (r/r_{200}) < 0.6$  (filled triangles with dotted line), and  $0.6 < (r/r_{200}) < 1.0$  (open circles with dashed-dotted line).

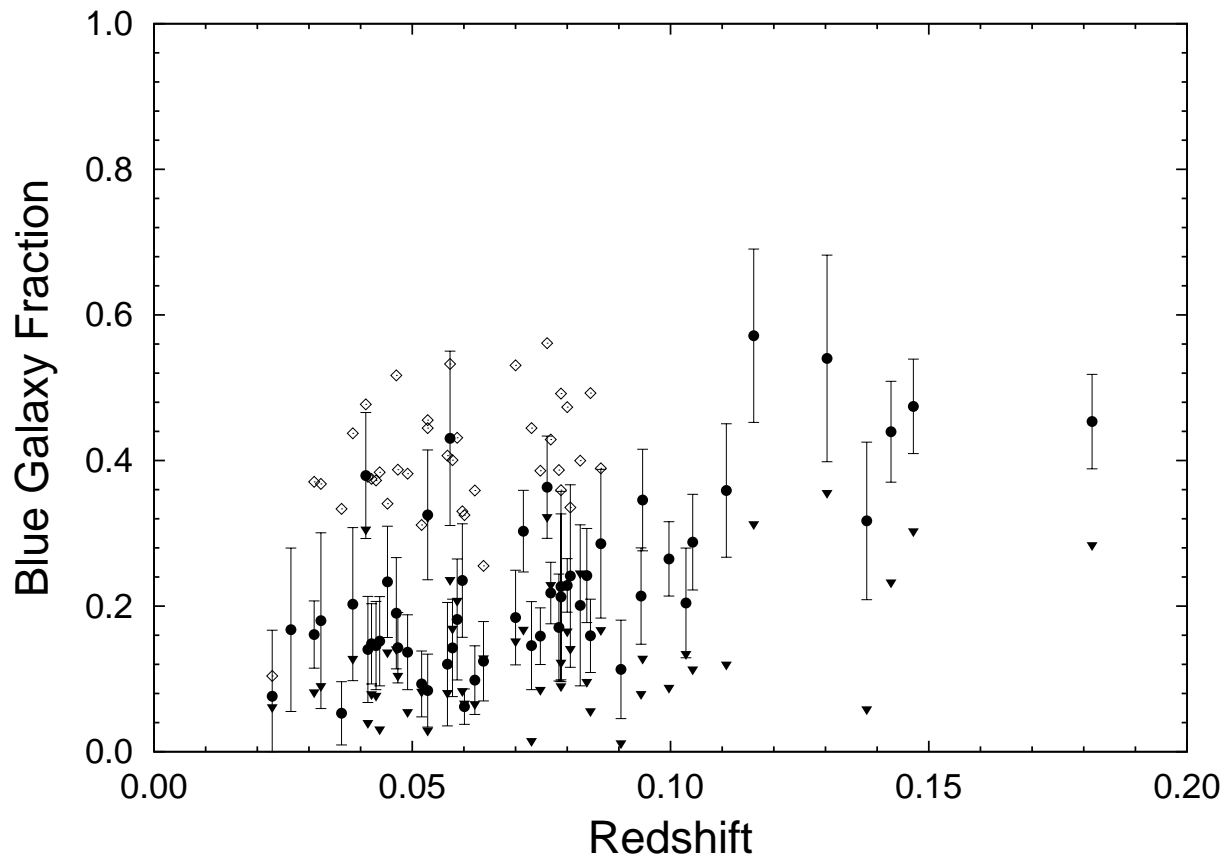


Fig. 6.— Redshift distribution of  $f_b$  for the cluster galaxy population that is 100% photometrically complete to  $M_{R_c} = -19$  (filled circles),  $M_{R_c} = -17$  (open diamonds), and  $M_{R_c} = -20.5$  (filled triangles). Error bars for the open symbols are similar to those for the filled symbols and have been omitted for clarity. The  $f_b$  has been measured for galaxies within a radius of  $(r/r_{200}) = 0.4$ .